Lawrence Berkeley National Laboratory

Lawrence Berkeley National Laboratory

Title

SMALL AREA SILICON DIFFUSED JUNCTION X-RAY DETECTORS

Permalink

https://escholarship.org/uc/item/5gn150k7

Author

Walton, J.T.

Publication Date

1981-10-01

Peer reviewed

Lawrence Berkeley Laboratory

UNIVERSITY OF CALIFORNIA

Engineering & Technical Services Division

SMALL-AREA SILICON-DIFFUSED JUNCTION X-RAY DETECTORS

J.T. Walton, R.H. Pehl, and A.E. Larsh

October 1981

J. T. Walton, R. H. Pehl and A. E. Larsh
Lawrence Berkeley Laboratory
University of California
Berkeley, California 94720 U.S.A.

Abstract

The low temperature performance of silicon dif-
fused junction detectors in the measurement of low
energy x-rays is reported. The detectors have an
area of $0.04cm^2$ and a thickness of $100\mu m$. The spec-
tral resolutions of these detectors were found to be
in close agreement with expected values indicating
that the defects introduced by the high temperature
processing required in the device fabrication were
not deleteriously affecting the detection of low
energy x-rays. Device performance over a temperature
range of $77°K$ to $150°K$ is given. These detectors were
designed to detect low energy x-rays in the presence
of minimum ionizing electrons. The successful appli-
cation of silicon diffused junction technology to
x-ray detector fabrication may facilitate the develop-
ment of other novel silicon x-ray detector designs.

Introduction

A proposal[1] to determine the elemental surface
composition of the four Galilean satellites of Jupiter
(Galileo Mission) by examining the emitted flux of
x-rays presents some novel instrumentation problems.
Since the instrument package must pass relatively
near the satellites (<3 radii) which are located in
the Jovian magnetosphere, the effects of the atten-
dant high flux of electrons ($\sim 10^8 cm^{-2}sec^{-1}$) must be
minimized. Further, the anticipated x-ray flux from
the satellites is relatively high ($\sim 10^5 cm^{-2}sec^{-1}$) and
to maintain the x-ray counting rate to practical
levels detectors with small areas should be employed.
Consequently, detectors of $4mm^2$ in area and $100\mu m$
thick were proposed to detect the x-rays of interest
(1-12keV).

The dimensions ($\sim 2.3mm$ diameter) of the proposed
detectors are such that conventional techniques for
silicon x-ray detector fabrication are difficult to
apply. The device size requirements are more readily
met by applying photolithographic techniques which are
used in the semiconductor circuits industry or which
have been used on occasion in the fabrication of dif-
fused junction radiation detectors.[2]

Diffused junction silicon detectors have been
employed for many years in the detection of high
energy particles in room temperature applications.
The high temperature processing required to fabricate
these devices can introduce deep level traps into the
silicon bandgap. While not appreciably affecting room
temperature performance for high energies, these deep
traps would normally preclude low temperature appli-
cations by trapping an appreciable fraction of the
signal charge carriers. However, since the proposed
detectors are only $100\mu m$ thick, we decided that a
sufficiently high electric field could be applied to
the devices to possibly move the charge carriers
across the detector depletion region without the
traps causing significant signal degradation.

On the proposed mission, operation of these
detectors at the highest temperature possible without
performance degradation is highly desirable. Mini-
mizing the detector leakage current is thus a very

important goal that we felt could best be obtained by
employing a guard-ring structure.[3] The desire to
detect low-energy x-rays requires that the devices
have very thin entrance windows. In the following,
we report our measurements on two different diffused
junction diode structures—a simple detector and a
detector with a guard ring, and two different entrance
window fabrication techniques—boron ion implantation
and metal silicide formation.[4]

Device Fabrication

The structure of a simple diffused junction
detector is shown in Fig. 1a, where the N^+ contact
is produced by the thermal diffusion of phosphor
into the p-type material through the opening in the
silicon dioxide layer. The P^+ contact is, for a
completely diffused device, a thermally diffused
boron layer. We have for some time employed either
boron ion implantation or metal silicides to form
this P^+ contact.
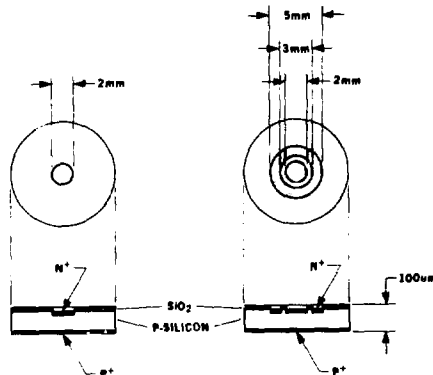
N⁺ CONTACT: PHOSPHORUS DIFFUSION

P⁺ CONTACT: BORON IMPLANTATION OR METAL SILICIDE

XBL 815-9723

Fig. 1. Simple diode (a) and guard-ring diode (b)
geometries employed on the detectors. The
N^+ and P^+ contact technologies are noted.

The wafers used to fabricate the detectors re-
ported here were cut from a crystal of vacuum-grown
p-type silicon with a resistivity of 4600 ohm-cm,
$500\mu sec$ minority carrier lifetime, [111] orientation
and 2000-3000 dislocations/cm^2. The wafers were
lapped and then chemically etched (20:1; HNO_3:HF)
to remove the lapping damage.

Our processing for diffused junction devices re-
quires the growth of silicon dioxide in steam at

1000°C for three hours. This produces an oxide layer of approximately 7000Å. Openings are then cut through this oxide layer using photomasking techniques. A phosphorus diffusion is performed at 950°C for 20 minutes. After removal of the oxide from the opposite side of the wafer, a boron ion implantation (25keV, 5×10^{13} ions/cm^2) followed by a 30-minute anneal at 750°C is used to form the P$^+$ contact. Alternatively we use palladium silicide (Pd$_2$Si) for the P$^+$ contact. This latter process involves a vacuum evaporation of palladium (500Å) onto the wafer and then heating of the wafer to 300°C for 30 minutes. Gold is evaporated onto both the N$^+$ and P$^+$ contacts to ensure good electrical conduction--approximately 500Å onto the N$^+$ contact and 200Å onto the P$^+$, the latter being the entrance window for the x-rays.

Measurements and Results

Room Temperature

The room temperature reverse leakage current, capacitance and noise (FWHM) as a function of the applied voltage for representative devices are shown in Figs. 2a and 2b. Noted on the figures are the depletion voltages at which ^{241}Am alphas are completely detected. The expected depletion voltage for 100μm thick detectors made from 4600 ohm-cm p-type silicon is 25 volts.[5] The values measured are considerably less than this indicating that the net impurity concentration $N_T = |N_A - N_D|$ (where N_A and N_D are the acceptor and donor concentrations in silicon respectively) has been altered by the process thermal cyclings. The expected capacitance for the devices is 4.4pF and the measured values are in good agreement with this. The room temperature alpha performance of guard-ring detectors with boron implanted and metal silicide P$^+$ contacts is shown in Figs. 3a and 3b.
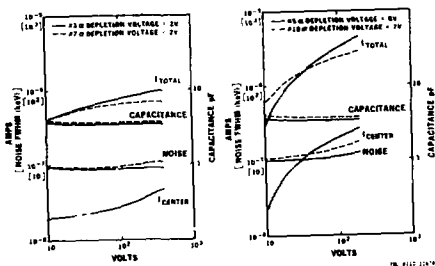

Fig. 2. Leakage current, noise and capacitance versus bias voltage for representative (a) boron ion implantation and (b) palladium silicide (Pd$_2$Si) P$^+$ contact detectors.

If the dominant trapping centers are at the middle of the energy bandgap, the expected 'eakage current, I_D, due to thermal generation is given by[5]:

$$I_D = \frac{qn_i X}{2\tau_p}$$

where $q = 1.6\times10^{-19}$ coulombs; n_i, the intrinsic carrier concentration, is 1.6×10^{10} carriers-cm^{-3}; X, the depletion volume in cm^3, is 4×10^{-4} cm^3; and τ_p, the minority carrier lifetime in seconds, is 500μsec for the starting material. If we assume that the leakage currents measured at low bias voltages in the central region of the guard-ring detectors are relatively free of surface leakage currents, then the preceeding equation can be used to estimate the minority carrier lifetime. The currents measured are approximately 3×10^{-8}A which yields a minority carrier lifetime in the finished detectors of 16μsec. The thermal cycling has therefore apparently reduced the lifetime from 500μsec to 16μsec.
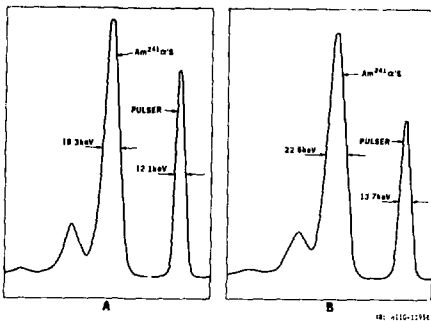

Fig. 3. Room temperature ^{241}Am spectra for (a) boron implantation and (b) palladium silicide (Pd$_2$Si) P$^+$ contact guard-ring detectors. The spectra were obtained with an amplifier having a Gaussian filter of 1μsec peaking time.

The effective entrance window thicknesses measured on these devices with ^{241}Am alphas by the angle of incidence technique[5] were found to be 0.3μm and 0.5μm for the boron implanted and metal silicide P$^+$ contacts respectively.

Cryogenic Measurements

The expected photo-efficiency for a silicon detector 100μm thick with an entrance window thickness of 0.3μm is shown in Fig. 4. Since the detector response is begining to decrease rapidly above 7keV, we used an ^{55}Fe source (5.9keV) in our x-ray measurements on these detectors. The detectors were tested in a cryostat with a pulsed-opto-electronic feedback system[6] shown schematically in Fig. 5. The field effect transistor (FET) is a low input capacitance (~5pF) 2N4416, which with a 17μsec filter peaking time amplifier and no capacitive load has about 90eV (FWHM) resolution and about 30eV/pF degradation in resolution with detector capacitance loading. Consequently with a detector capacitance of 4pF, we would expect an electronic noise resolution of approximately 210eV (FWHM). The measured ^{55}Fe spectrum on one of our guard-ring detectors is shown in Fig. 6.

We have used this system to evaluate silicon x-ray detectors which are normally operated at or near liquid nitrogen (LN$_2$) temperatures.
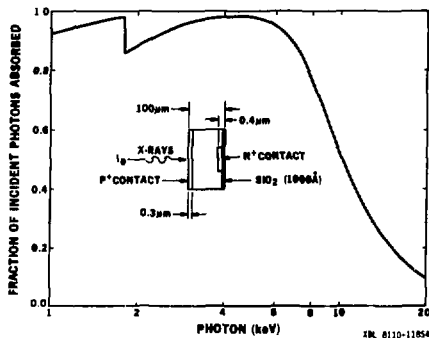
Fig. 4. Theoretical fraction of incident photons detected in a 100 μm thick silicon detector with an 0.3 μm entrance window.

The FET temperature has been adjusted to give optimum resolution when the module in Fig 5 is cooled to LN$_2$ temperatures. For the tests reported here, we allowed the entire module to operate over the temperature range from 77°K to ~200°K. Therefore the FET which operated at its optimum noise point when the module was at the coldest temperature was not thermally optimized when the module was warmed. This contributes about 5-10eV to our measurements at 170°K.
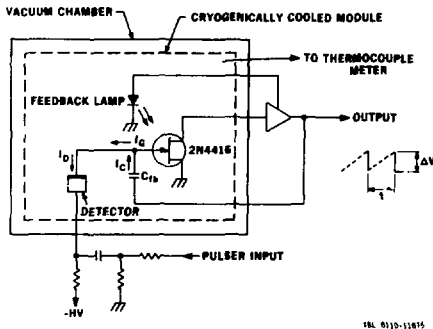

Fig. 5. A simplified diagram of the pulsed-opto-electronic feedback system used to measure the x-ray performance of the detectors. The entire module, FET and detector, was thermally cycled for the temperature measurements.

The detector leakage current can be estimated from the preamplifier reset rate of the pulsed-opto-electronic feedback system assuming that the FET gate leakage current, I_G, is less than the detector leakage current, I_D, i.e. at the gate node:

$$I_D - I_G = I_C$$

$$I_D = I_C \text{ if } I_D \gg I_G$$

and:

$$I_C = \frac{C_{fb} \Delta V}{t}$$

where in Fig. 5, C_{fb} is the feedback capacitor and ΔV is the output voltage swing between resets of period t. However for our guard-ring devices at 20-30 volts bias, the detector leakage current and FET gate leakage currents are comparable making an accurate estimate of the detector leakage current difficult. This is illustrated in Fig. 7a which shows the resolution and leakage current as a function of temperature for boron implanted P$^+$ contact devices. For the guard ring device with 30 volts applied the system ceased to operate at 160°K due to the gate current exceeding the detector leakage current; increasing the detector bias voltage to 80 volts increased the detector leakage current sufficiently to allow operation to ~200°K. Figure 7b shows the comparable performance of the metal silicide P$^+$ contact devices.

If the detector leakage current is produced by band-to-band transitions, the current is expected to have a temperature dependence as given below:[7]

$$I_D \alpha T \exp\left(\frac{-E_g}{kT}\right)$$

where T is the temperature in °K, $k = 8.65 \times 10^{-5}$ eV/°K, and E_g is the bandgap energy in eV. The temperature dependence of the T term can be ignored in our measurements and a plot of ln I_D versus 1/T will yield the bandgap energy as the slope. A plot of the leakage current versus 1/T for four different devices is shown in Fig. 8. The average slope is 0.2eV, indicating that generation across the bandgap is not the limiting current generation mechanism.

In addition to measuring spectral resolution on our detectors, we normally measure the percentage of counts that are not completely collected and consequently fall into the background below the spectral peak. While we do not completely understand all the contributing factors to this background[8], we have experimentally established some criteria for assessing a detector's performance. For an ^{55}Fe spectrum we integrate the number of counts falling in certain fraction of the background below the peak and then divide this number by the total number of counts appearing in the peak. We nominally attain a value for the ratio:

$$\frac{\text{counts in background}}{\text{counts in peak}} < 8 \times 10^{-3}.$$

We suspect that detectors with values greater than this have entrance window and/or surface state problems. The x-rays stopping in the windows produce charge signals which can slowly diffuse into the detector active region and be collected. The charge from the x-rays stopping near the surface region will also be slowly collected. For the diffused junction detectors measured here the background-to-peak ratio was of the order of 20×10^{-3} irrespective of the device geometry or the P$^+$ contact fabrication technique which suggests that signal charge is being collected off the silicon/silicon dioxide surface.

Discussion

The absence of any detectable trapping in the ^{55}Fe spectra indicates that the density of traps present in the material initially or induced by the thermal processing is sufficiently low that their effects can
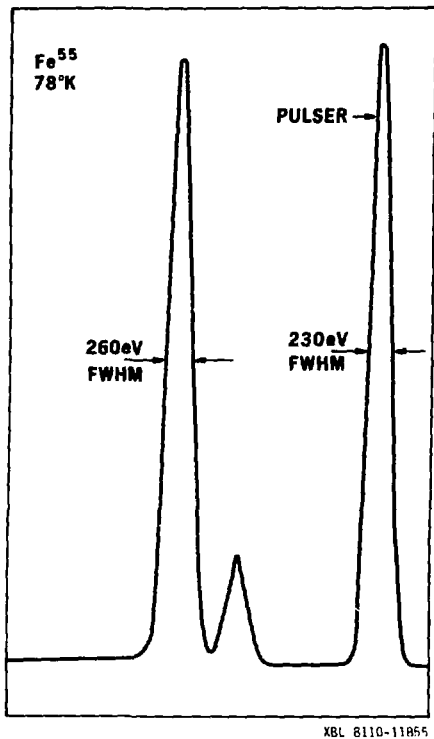
-3-

Fe^{55}
78°K

PULSER →

260eV FWHM ← → 230eV FWHM

Fig. 6. An ^{55}Fe spectrum obtained on a diffused junction guard-ring detector. A spectral resolution of 260 eV (FWHM) and an electronic resolution of 230 eV (FWHM) was obtained with an amplifier having a Gaussian filter of 17 µsec peaking time.

be overcome by the applied electric field. The field employed here is approximately a factor of five greater than that normally employed with lithium drifted silicon, Si(Li), detectors (i.e. 5000V/cm versus 1000V/cm). The higher field coupled with the thin devices reduces the probability that the signal charge carriers will interact with a trap; this was the basis for our proposal to use diffused junction devices for the Galileo Mission. The ^{55}Fe results, as shown in Fig. 6, have substantiated this model.

The leakage current variation as a function of temperature is larger than anticipated. The measured thermal activation energy of about 0.2eV associated with this leakage current is considerably less than the known bandgap energy of 1.1eV for silicon. We assume that this current is due to currents generated in the silicon/silicon dioxide interface since the bulk currents cannot be responsible. Bulk currents would almost certainly be dominated by mid-band traps providing a two-step transition of electrons from the valence band to the conduction band. This would result in an activation energy of 0.55eV for silicon.

Consequently, the leakage current temperature performance here must be due to silicon/silicon dioxide surface leakage currents. Further, the electrical activity of the surfaces is also perhaps indicated by the high x-ray background observed, which could be attributed to charge signals being collected off the silicon/silicon dioxide interface. However additional work is required to confirm this.

The leakage current temperature performance of these devices limits their application to temperatures of less than 190°K. It would be desirable, not only for the Galileo mission but for other applications, to be able to operate at higher temperatures. Oxide-passivated junction detectors with room temperature leakage currents which are approximately two orders of magnitude less than our devices have been recently reported by Kemmer.[9] This improvement is attributed to modifications in the fabrication techniques which resulted in the minority carrier lifetime being increased and the surface leakage current being eliminated by the process schedule. Consequently these process improvements may result in detectors which will operate satisfactorily over a wider temperature range than reported here. In addition, the improvements may yield devices where the x-ray background is also reduced.

There is only a small difference between the performance of the boron implantation and palladium silicide P^+ contacts at cryogenic temperatures. The device performance is being dominated by the surface leakage current and a quantitative analysis of the differences in these two contact formation techniques will have to await an improvement in this current.

Conclusions

These results demonstrate the feasibility of using diffused junction detectors for low energy x-ray analysis over an extended range of cryogenic temperatures. The present guard-ring detector is very close to being suitable for the Galileo mission. Process improvements, however, may yield devices capable of operating at higher temperatures than reported here.

The use of silicon diffused technology opens the possibility of some rather novel geometrical designs for low energy x-ray detection. For example, an array of small elements which would allow low-energy x-ray imaging would be possible with the device technology described in this paper. Further, the incorporation of the FET and detector into one structure for low energy applications appears feasible.

Acknowledgements

Fig. 8. Leakage current for four different detectors versus $1/T$ ($°K^{-1}$) indicating an average slope of 0.2 eV.
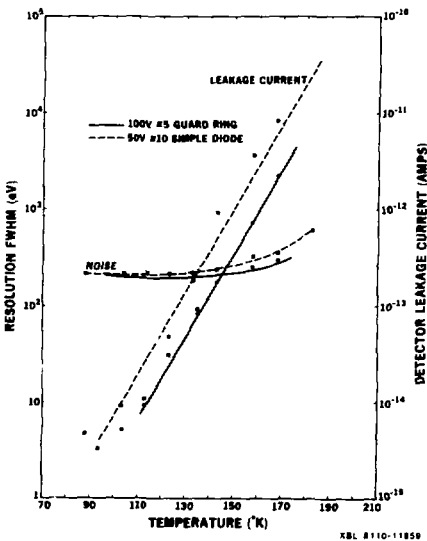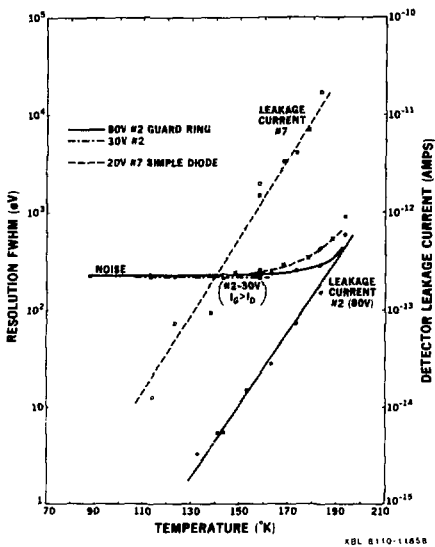

Fig. 7. Noise (FWHM) obtained with an amplifier having a Gaussian filter of 17μsec peaking time and leakage current versus temperature (°K) for (a) boron ion implanted and (b) palladium silicide P$^+$ contact detectors.
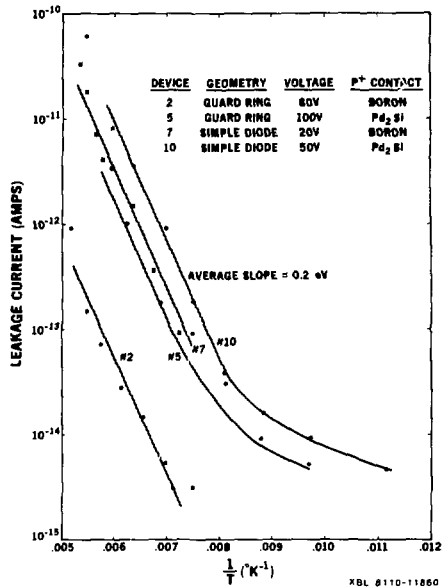
References

1. Metzger A E, Surface Composition of the Galilean Satellites by Encounter X-Ray Spectroscopy, 2000-15, Jet Propulsion Laboratory, California Institute of Technology, Pasadena, California 1976.

2. Hansen W L and Goulding F S, Nucl. Inst. and Meth. 29, 345 (1964).

3. Goulding F S and Hansen W L, Nucl. Inst. and Meth. 12, 249 (1961).

4. Kircher C J, Solid State Electron. 14, 507 (1971).

5. Coche A and Siffert P, Semiconductor Detectors, Ch. 2, eds. Bertolini G and Coche A, North Holland Publ. Co., Amsterdam (1968).

6. Landis D A, Goulding F S and Jarrett B V, Nucl. Inst. and Meth. 101, 127 (1972).

7. Pehl R H, Haller E E and Cordi R C, IEEE Trans. Nucl. Sci. NS-20, No. 1, 494 (1973).

8. Goulding F S, Nucl. Inst. and Meth. 142, 213 (1977).

9. Kemmer J, Nucl. Inst. and Meth. 169, 499 (1980).